Received: 28 March 2024 | Revised: 27 June 2024 | Accepted: 2 July 2024

DOI: 10.1111/ppl.14483

ORIGINAL RESEARCH

Physiologia Plantarum

A salicylic acid-associated plant-microbe interaction attracts beneficial *Flavobacterium* sp. to the *Arabidopsis thaliana* phyllosphere

Anna Sommer[1,2] | Marion Wenig[2] | Claudia Knappe[2] | Susanne Kublik[3] | Bärbel U. Foesel[3] | Michael Schloter[3,4] | A. Corina Vlot[1,2]

[1]Faculty of Life Sciences: Food, Nutrition and Health, Chair of Crop Plant Genetics, University of Bayreuth, Kulmbach, Germany

[2]Helmholtz Zentrum Muenchen, Institute of Biochemical Plant Pathology, Neuherberg, Germany

[3]Helmholtz Zentrum Muenchen, Institute for Comparative Microbiome Analysis, Neuherberg, Germany

[4]Chair for Environmental Microbiology, Technische Universität München, Freising, Germany

Correspondence
A. Corina Vlot,
Email: corina.vlot@uni-bayreuth.de

Funding information
Deutsche Forschungsgemeinschaft, Grant/Award Number: SPP 2125

Edited by P. Poór

Abstract

Both above- and below-ground parts of plants are constantly challenged with microbes and interact closely with them. Many plant-growth-promoting rhizobacteria, mostly interacting with the plant's root system, enhance the immunity of plants in a process described as induced systemic resistance (ISR). Here, we characterized local induced resistance (IR) triggered by the model PGPR *Pseudomonas simiae* WCS417r (WCS417) in *Arabidopsis thaliana*. Hydroponic application of WCS417 to *Arabidopsis* roots resulted in propagation of WCS417 in/on leaves and the establishment of local IR. WCS417-triggered local IR was dependent on salicylic acid (SA) biosynthesis and signalling and on functional biosynthesis of pipecolic acid and monoterpenes, which are classically associated with systemic acquired resistance (SAR). WCS417-triggered local IR was further associated with a priming of gene expression changes related to SA signalling and SAR. A metabarcoding approach applied to the leaf microbiome revealed a significant local IR-associated enrichment of *Flavobacterium* sp.. Co-inoculation experiments using WCS417 and *At*-LSPHERE *Flavobacterium* sp. Leaf82 suggest that the proliferation of these bacteria is influenced by both microbial and immunity-related, plant-derived factors. Furthermore, application of *Flavobacterium* Leaf82 to *Arabidopsis* leaves induced SAR in an NPR1-dependent manner, suggesting that recruitment of this bacterium to the phyllosphere resulted in propagation of IR. Together, the data highlight the importance of plant-microbe-microbe interactions in the phyllosphere and reveal *Flavobacterium* sp. Leaf82 as a new beneficial promoter of plant health.

1 | INTRODUCTION

The functional traits introduced by the plant-associated microbiome are essential for plant growth and fitness and include nutrient acquisition as well as improved responses of the plant towards abiotic and biotic stressors (Schlaeppi & Bulgarelli, 2015; Müller et al., 2016; Sohrabi et al., 2023). Some microbes can activate plant defence mechanisms, including mechanisms known as systemic acquired resistance (SAR) and induced systemic resistance (ISR). While SAR is induced in systemic tissues of plants undergoing a local pathogen infection, ISR is induced in aerial tissues of plants in response to interactions of the roots with beneficial microbes in the rhizosphere (Pieterse et al., 2014; Vlot et al., 2021; Zhu et al., 2022).

SAR relies on two distinct but interwoven signalling pathways, one depending on salicylic acid (SA), and the other on pipecolic acid (Pip) (Hartmann & Zeier, 2019; Nair et al., 2021; Vlot et al., 2021; Yildiz et al., 2021; Zeier, 2021; Yildiz et al., 2023). SA levels rise both locally and systemically after pathogen infection. This is driven by the enzymes ISOCHORISMATE SYNTHASE 1 (ICS1, also known as SID2) followed by the amidotransferase AvrPphB SUSCEPTIBLE3 (PBS3) (Wildermuth et al., 2001; Rekhter et al., 2019). Elevated SA levels lead to enhanced resistance through the action of downstream signalling intermediates, including the proposed SA receptors NON-EXPRESSOR OF PATHOGENESIS-RELATED PROTEINS1 (NPR1) and its paralogs NPR3 and 4 (Fu et al., 2012; Ding et al., 2018; Liu et al., 2020; Wang et al., 2020; Zavaliev et al., 2020; Zavaliev & Dong, 2024). In parallel, the non-proteinogenic amino acid Pip is synthesized in two steps by AGD2-like DEFENCE RESPONSE PROTEIN 1 (ALD1) and SAR-DEFICIENT 4 (SARD4) and then converted by FLAVIN-DEPENDENT MONOOXYGENASE 1 (FMO1) to its presumed bioactive form *N*-hydroxy-pipecolic acid (NHP) (Návarová et al., 2012; Ding et al., 2016; Hartmann et al., 2017; Chen et al., 2018; Hartmann et al., 2018). FMO1 is suspected to tightly regulate NHP levels during systemic immunity events together with UDP-GLYCOSYL TRANSFERASE 76B1 (UGT76B1), which glycosylates NHP, rendering it inactive (Bauer et al., 2021; Cai et al., 2021; Holmes et al., 2021; Mohnike et al., 2021; Eccleston et al., 2022).

The long-distance signal, which mediates the communication between local infected and systemic tissues and ultimately triggers the establishment of SAR, appears to be composed of multiple signalling intermediates, including the C9 dicarboxylic acid azelaic acid, glycerol-3-phosphate, and NHP (Jung et al., 2009; Chanda et al., 2011; Cecchini et al., 2015; Lim et al., 2016; Chen et al., 2018; Wang et al., 2018; Holmes et al., 2021; Vlot et al., 2021; Yildiz et al., 2021). Additionally, volatile signals such as the monoterpenes camphene and α- and β-pinene are essential for SAR and propagate systemic immunity in SAR-induced as well as neighbouring plants (Riedlmeier et al., 2017; Wenig et al., 2019). GERANYL GERANYL DIPHOSPHATE SYNTHASE 12 (GGPPS12) is a key enzyme in the production of volatile monoterpenes in *Arabidopsis thaliana*. Mutations in this gene reduce monoterpene emissions and the capacity of the volatile emissions of these plants to support SAR (Riedlmeier et al., 2017; Wenig et al., 2019).

ISR is elicited by plant growth-promoting bacteria or fungi in the rhizosphere (PGPR/PGPF), including, for example, several *Pseudomonas*, *Bacillus*, and *Trichoderma* strains (reviewed in (Pieterse et al., 2014; Gill et al., 2016; Newitt et al., 2019; Vlot et al., 2021; Khan et al., 2022)). In contrast to SAR, which provides protection against (hemi-) biotrophic pathogens, ISR protects above-ground tissues against both necrotrophic and (hemi-) biotrophic pathogens. The best-characterized ISR to date is that induced in *Arabidopsis thaliana* upon an interaction of the roots with *Pseudomonas simiae* WCS417r (Pieterse et al., 1996; Pieterse et al., 2021). The traditional idea is that ISR depends on functional jasmonic acid (JA)-dependent plant defences (Pieterse et al., 1998; Ton et al., 2002; Pozo et al., 2008). However, evidence is accumulating that there is no uniform ISR response to all PGPR/Fs. Instead, there seem to be differing responses, depending on the eliciting microbial strains, involving JA signalling as well as SA signalling pathways (Niu et al., 2011; van de Mortel et al., 2012; Martínez-Medina et al., 2013; Cecchini et al., 2015; Nie et al., 2017; Wu et al., 2018; Shine et al., 2019). These different responses are believed to enable the plant to react in a directed manner depending on the lifestyle of the attacking pathogen (Nguyen et al., 2020; Nguyen et al., 2022). Therefore, we follow De Kesel and colleagues (Kesel et al., 2021) and refer to ISR as systemic IR.

The plant immune system influences the propagation of pathogens, but also that of non-pathogenic commensal or plant growth-promoting microbes, which are associated with the plant and together make up the plant microbiome (Hacquard et al., 2017; Teixeira et al., 2019; Stassen et al., 2021; Sohrabi et al., 2023). Leaf-to-root signalling in response to infection further mediates changes in root exudates that influence the composition of the rhizosphere microbiota, which is believed to result in a fortification of plant immunity against pathogens through systemic IR (Rudrappa et al., 2008; Berendsen et al., 2018; Stringlis et al., 2018; Stassen et al., 2021; Chen & Liu, 2024). The phyllosphere microbiome also responds to changes in the plant immune status (Chen et al., 2020; Chaudhry et al., 2021; Pfeilmeier et al., 2021; Sohrabi et al., 2023; Pfeilmeier et al., 2024). Not only pathogens but also commensal bacteria from the phyllosphere have been shown to enhance, for example, SA-associated immunity (Vogel et al., 2016). It thus seems conceivable that the plant immune system can modulate the phyllosphere microbiome, allowing the plant to 'exploit' beneficial properties of microbes to promote plant fitness.

In this study, we show that IR-associated responses of the plant microbiome are influenced by interconnected microbe-microbe and microbe-plant interactions. Reduced species diversity in response to *P. simiae* WCS417r inoculation indicates a potential impact on the stability of the leaf microbiome, while the data further highlight the importance of tri-partite plant-microbe-microbe interactions for plant health.

2 | MATERIALS AND METHODS

2.1 | Plant material and growth conditions

In this study, *Arabidopsis* ecotype Columbia-0 (Col-0) was used for all experiments. The mutants *ggpps12*, *ald1*, *npr1-1*, *sid2-1*, and *jasmonate-insensitive 1* (*jin1*) were previously described (Berger et al., 1996; Cao et al., 1997; Wildermuth et al., 2001; Song et al., 2004; Breitenbach et al., 2014; Riedlmeier et al., 2017; Wenig et al., 2019). Plants were grown from synchronised seeds using potting soil ("Floradur® B Seed", Floragard GmbH) mixed with silica sand (grain size 0,6–1,2 mm) at a ratio of 5:1. For IR experiments seeds were surface-sterilized with 75% ethanol twice for 4 min and grown on ½ Murashige and Skoog medium for

10 days (d) prior to treatment and transfer to soil. Plants were grown in a 10-hour (h) daylight regime and a light intensity of 100 µmol m^{-2} s^{-1} photosynthetically active photon flux density at 22°C during light periods and 18°C during dark periods. Relative humidity was kept at >70%.

2.2 | IR elicitors, pathogens and treatments

IR was elicited using *Pseudomonas simiae* WCS417r (WCS417) (Pieterse et al., 1996). Bacteria were grown on NB (Carl Roth, Karlsruhe, Germany) plates for 24 h and suspended in 10 Mm $MgCl_2$ to a final OD_{600} of 0.2. To induce IR, the roots of 10-day-old, sterile-grown seedlings were placed in wells of 96-well plates containing the bacterial suspension or a sterile 10 mM $MgCl_2$ control solution, each supplemented with 0.01% Tween-20 (v:v). After 1 h of incubation, the seedlings were placed in pots with soil and grown to an age of 34 d. On the 34th day after sowing, the third and fourth true leaves of the plants were either harvested for RT-qPCR or amplicon sequencing analysis or inoculated with 10^5 cfu mL^{-1} of *Pseudomonas syringae* pathovar *tomato* (*Pst*), which was maintained and used for analysis of infection severity as previously described (Wenig et al., 2019). Bacterial titres were determined in three replicate samples, including 3 leaf discs, each taken from at least 4–6 plants per biologically independent replicate experiment. The bacteria were extracted from the leaf discs, and colony-forming units (cfu) were counted in plate-based assays as described (Wenig et al., 2019). Biologically independent replicate experiments were performed in independently grown and treated plant batches.

To evaluate the adherence of WCS417 to roots as well as its uptake into leaves, plants were treated with WCS417 as described above and planted into potting soil. After 5 min, 1 h and 1 d, plants were removed from the soil and cut to separate roots and leaves. Roots as well as leaves were shaken in 10 mM $MgCl_2$ + 0,01% Silwet (v:v) for 1 h at 600 rpm. Subsequently, serial dilutions were made and plated as described (Wenig et al., 2019) on NYGA plates with 50 mg L^{-1} rifampicin to select for WCS417, which is naturally resistant to rifampicin (Pieterse et al., 1996). Two d later, bacterial titres were calculated based on the number of bacterial colonies formed.

In addition to WCS417, we also implemented *Flavobacterium* sp. in our studies. We used *Flavobacterium* strain Leaf82 from the *At*-LSPHERE synthetic community (Bai et al., 2015), which was maintained on NB medium. Leaf inoculations were performed using 4-5-week-old plants by syringe infiltration of a bacterial suspension ($OD_{600} = 0.0002$) in 10 mM $MgCl_2$. *In planta* bacterial titres were determined as described above by counting plate-grown bacterial colonies derived from leaf discs taken from inoculated leaves. Each biologically independent replicate was performed with a minimum number of 3 internal replicates, including 3 leaf discs each, and biologically independent replicates were performed using independently grown and treated plant batches. Colonies of WCS417 and Leaf82 were distinguished based on colour differences: WCS417 forms opaque, white colonies, and Leaf82 forms opaque orange colonies.

SAR was induced in 4-5-week-old plants as previously described (Wenig et al., 2019), except that Leaf82 was used for the primary inoculation of the first two true leaves of the plants by syringe infiltration of a bacterial suspension with an OD_{600} of 0.02 in sterile 10 mM $MgCl_2$. The same concentration of *Pst* carrying the effector *AvrRpm1* was used as the positive control, and 10 mM $MgCl_2$ was used as the negative control treatment (Wenig et al., 2019). Three d later, the establishment of SAR was tested by a secondary infection of the third and fourth true leaf of the plants with 10^5 cfu mL^{-1} of *Pst*, titres of which were determined at 4dpi as described (Wenig et al., 2019).

2.3 | Bacterial confrontation assay

The bacterial confrontation assay was performed on NB-agar. A vertical line of one bacterium was streaked with a heat-sterilised loop directly onto the agar. The second bacterium was applied as a perpendicular line with a heat-sterilised infection loop on top of the other. The bacteria were grown at 25°C for two days.

2.4 | RNA extraction and RT-qPCR analysis

RNA was isolated with Tri-Reagent (Sigma-Aldrich) according to the manufacturer's instructions. cDNA was generated with Superscript II reverse transcriptase (Invitrogen, Carlsbad, USA). Quantitative PCR (qPCR) was performed using the Sensimix SYBR low-rox kit (Bioline) on a 7500 real-time PCR system (Applied Biosystems). Primers that were used for qPCR are listed in Table S1. Transcript accumulation of target genes was analysed using Relative Quantification with the 7500 Fast System Software 1.3.1.

2.5 | Statistical analysis of bacterial titre and RT-qPCR data

All statistical analyses were done using R version 3.6.3. (R Development Core Team, 2020). For the analysis of bacterial titres, a Shapiro Wilk test for normal distribution showed that the cfu counts resulting from the infection assays did not follow normal distribution ($\alpha = 0.01$). Therefore, a Kruskal-Wallis test was used to test for significance at $\alpha = 0.05$. Regarding the SAR experiments, a paired samples Wilcoxon test was performed as a post-hoc test for the different treatments (Wilcoxon, 1945). For the analysis of the primed states of genes, the highest RQ value amongst the time points 2, 4, and 6 hpi was taken per experiment and treatment. The corresponding values were statistically compared to the corresponding T0-values, and the control-sample value was set to 1. Since a normal distribution was not given, we tested for significant differences between the RQ according to treatment with a Kruskal-Wallis test.

2.6 | DNA-Isolation, PCR and amplicon sequencing

For each individual DNA sample, one leaf per plant, either the 3rd or 4th true leaf, in total 10 plants per treatment were harvested and pooled. This corresponded to 100–200 ng of leaf material per sample, which was freeze-dried for 24 h at −40°C and 0.12 mbar (Alpha 2–4 LD Plus, Martin Christ Gefriertrocknungsanlagen). Replicate samples were harvested from biologically independent experiments performed in independently grown and treated plant batches. DNA isolation was performed utilizing the FastPrep Soil Kit (Mpbio) according to the manufacturer's instructions after an additional step of leaf grinding using a tissue lyser (Retsch) and glass beads (1 mm diameter) at 25 Hz for 2 min. Following DNA extraction, the variable regions V5-V7 of the bacterial 16S rRNA gene were amplified by PCR (NEBnext High Fidelity 2x Master Mix, New England Biolabs) using 10 ng of DNA per reaction and the primers 799F and 1193R from (Chelius & Triplett, 2001; Bulgarelli et al., 2012).

Three independent PCR reactions were performed per DNA sample using the following conditions: 98°C for 30 s, 98°C for 10 s, 58°C for 20 s, 72°C for 20 s, 72°C for 2 min. Steps 2–4 were repeated 25 times. The resulting PCR amplicons were subjected to gel electrophoresis with an agarose concentration of 1.5% to separate amplicons derived from bacteria and chloroplasts since chloroplast DNA yields longer amplicons than bacterial DNA. The DNA amplicons derived from the bacterial 16S rRNA gene were extracted from the gels using the QIAquick Gel Extraction Kit (Qiagen). After determination of the DNA concentration of each PCR reaction (Nanodrop, Implen), the 16S rRNA gene amplicons from 3 replicates per sample were pooled at equimolar amounts. The fragment sizes and concentrations of the pooled samples were determined on a Fragment Analyzer 5200 using the DNF-473-Standard Sensitivity NGS Fragment Analysis Kit (Agilent). The indexing PCR was performed under the following conditions: 98°C for 10 s, 55°C for 30 s and 72°C for 30 s and final extension at 72°C for 5 min. Each PCR reaction contained 1x NEBNext High Fidelity Mastermix, 10 ng of template DNA and index primer 1 (N7xx) and index primer 2 (N5xx) of Nextera XT Index Kit v2 Set A (Illumina) according to the manufacturer's instructions. All samples were purified using MagSi NGSprep Plus Beads (Steinbrenner). Samples were validated and quantified on a Fragment analyzer 5200 using the DNF-473-Standard Sensitivity NGS Fragment Analysis Kit, diluted and pooled to a final concentration of 4 nM for the sequencing run on an Illumina MiSeq using the MiSeq Reagent Kit v3 (600-cycle). Demultiplexing was done using the MiSeq Reporter Software v 2.6. (Illumina).

2.7 | Amplicon sequencing-data analysis

Pre-processing of the amplicon data was performed using the package "dada2", including trimming, removal of low-quality reads, merging of reads, chimaera removal and taxonomic assignment based on the Silva Seeds v.138 database (Yilmaz et al., 2014; Callahan et al., 2016). The reads were truncated at the first occurrence of a quality score ≤2. Filtering criteria were a length of at least 270 bp in forward reads, and 150 bp in reverse reads and the absence of ambiguous bases in the remaining reads. In total, 718,990 reads were processed in 14 samples and after preprocessing 508,154 reads remained, which were assigned to taxons based on Amplicon Sequence Variants (ASVs). This resulted in 1,434 unique ASVs. ASVs belonging to the Phylum "Cyanobacteria" were considered plant chloroplast-derived contaminants and removed before proceeding with further analysis. ASVs comprising less than 0.005% of all reads were also removed from the dataset. After those steps, 866 ASVs remained.

Prior to further analysis of the data, we controlled the *Pst* titre reductions triggered by each treatment as compared to the appropriate controls. This was done to check whether IR was elicited; data from samples derived from experiments in which the WCS417 treatment did not significantly reduce *Pst* titres were excluded from further analysis. Data from the remaining 6–7 replicates per treatment were analysed using the R packages Vegan, Phyloseq and DESeq2 (Dixon, 2003; McMurdie & Holmes, 2013; Love et al., 2014; Schliep et al., 2017). Visual inspection of rarefaction curves indicated a sufficient sequencing depth (Supplementary Figure S1).

Alpha diversity was calculated using Shannon's- as well as Simpson's index (SIMPSON, 1949; Spellerberg & Fedor, 2003). Statistically significant differences in alpha-diversity were calculated utilizing a pairwise t-test since a previous Shapiro–Wilk test did not show any indication of a deviation of normality. Analysis of the obtained data indicated one outlier sample per treatment. This was confirmed by a Grubbs' test (Grubbs, 1950), which was significant for the number of observed ASVs for the respective samples of both treatments, near significant (WCS417) or significant (control) regarding the Shannon's, and significant for the sample from the control-treatment regarding the Simpson's Index. This concerns the samples control treatment, replicate 2 and WCS417 treatment, replicate 6. Those were removed from the dataset preceding further analysis (p-values of Grubb's test, see Supplementary Table S2).

To address β diversity, the R package "DESeq2" was used: the data were transformed using the built-in function in DESeq2 by calling "variancestabilizingTransformation" (McMurdie & Holmes, 2014), and subsequently, a PCA was fitted using "plotPCA." Based on the resulting distance matrix, a MANOVA was performed to test for significant differences in the overall microbial community dependent on the treatment (Love et al., 2014; Pfeilmeier et al., 2021).

Differentially abundant ASVs were also determined using DESeq2 (Love et al., 2014; Pfeilmeier et al., 2021). The analysis was limited to ASVs present in at least three replicates; ASVs were considered as differentially abundant with an FDR-corrected p-value <0.05.

3 | RESULTS

3.1 | *Pseudomonas simiae* WCS417r propagates in the phyllosphere of *Arabidopsis thaliana*

P. simiae WCS417r, referred to below as WCS417, triggers systemic IR in *Arabidopsis*, reducing the propagation of pathogenic *P. syringae*

pathovar *tomato* (*Pst*) in the leaves of the treated plants (Pieterse et al., 1996). To trigger systemic IR, WCS417 is applied to the soil surrounding *Arabidopsis* roots. Here, we investigated whether WCS417 also induces resistance when applied to plants by alternative methods. To this end, we treated 10-day-old, sterile-grown seedlings by dipping their roots in a WCS417 suspension. Subsequently, plants were transferred to soil. Because we detected viable WCS417 bacteria in the phyllosphere of the treated plants, we first investigated a possible propagation of WCS417 in *Arabidopsis* roots and leaves. To this end, we treated *Arabidopsis* plants with WCS417 via root-dip inoculation and transferred the treated plants to soil one hour later. After 5 min, 1 h and 1d, the plants were removed from the soil and the WCS417 titres were assessed in root and leaf tissues in a plate-based assay, using rifampicin to select for WCS417 (Pieterse et al., 1996). WCS417 titres were lower in the leaves than in the roots but were evident from the first sampling time point (Figure 1A). The roots were colonized in high numbers (>1x10^3 cfu per sample) from the first timepoint, with the highest values detected 1 h after transfer of the treated plants to soil. Similarly, WCS417 titres reached a maximum in the leaves at 1 h after transfer to soil and were reduced to 1x10^4 cfu per sample 1d later (Figure 1A).

While uptake of *Pseudomonas* spp. through the xylem cannot be excluded (Misas-Villamil et al., 2011; Kong et al., 2020; Paauw et al., 2023), it is equally possible that bacteria spread from the roots to the leaves via capillary water movement on the surface of the hypocotyl. When treated by root-dip with iodine-stained water, *Arabidopsis* seedlings take up most of the dye via capillary water movement on the surface of the hypocotyl (Figure S2). Next, we investigated whether WCS417 propagates in the phyllosphere of *Arabidopsis*. To this end, we inoculated leaves with 10^5 cfu mL^{-1} of WCS417 by syringe infiltration and determined the resulting bacterial titres 2 h (0 dpi) and 6 d later. As a positive control, we included *Pst*, which carried the effector *AvrRpm1*. Although the avirulent, pathogenic control bacteria *Pst/AvrRpm1* grew to higher titres, we detected a significant increase in WCS417 titres at 6 dpi as compared to 0 dpi, indicating active proliferation of WCS417 in *Arabidopsis* leaves (Figure 1B). Thus, root-dip inoculation of roots of *Arabidopsis* seedlings resulted in the uptake of bacteria via capillary movement of the inoculum on the surface of the hypocotyl and subsequent proliferation of WCS417 in the phyllosphere.

3.2 | WCS417 elicits local induced resistance in the *Arabidopsis* phyllosphere

In the following experiment, we studied whether root-dip inoculation of *Arabidopsis* with WCS417 enhanced the resistance of the leaves to pathogenic *Pst*. As described above, the roots of 10-day-old, sterile-

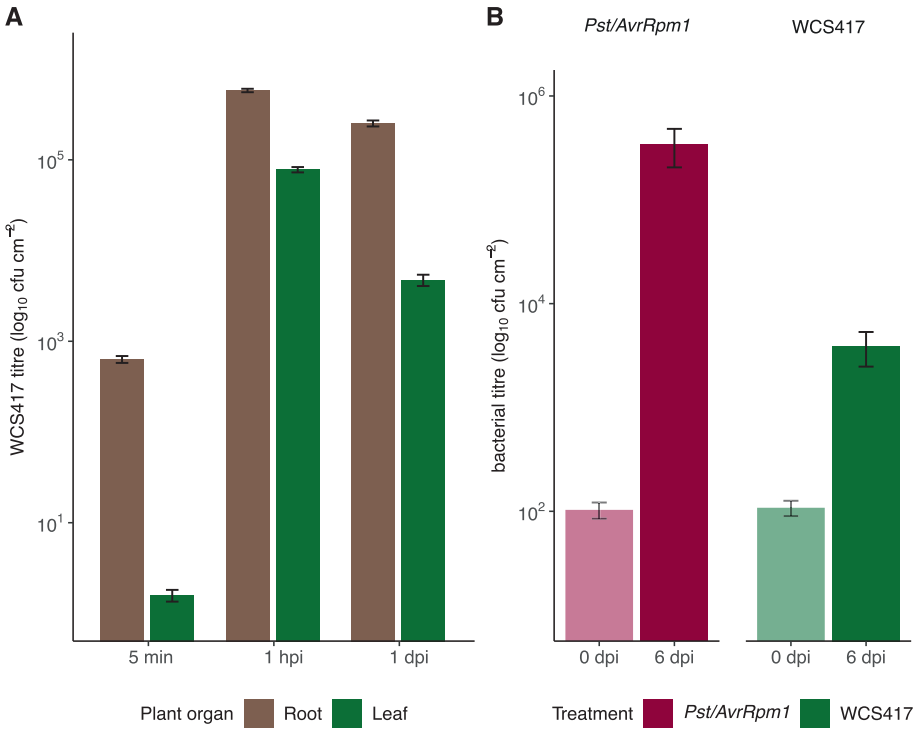

FIGURE 1 Proliferation and mobility of *P. simiae* WCS417r (WCS417) on *Arabidopsis thaliana* plant organs. **(A)** Adherence and proliferation of WCS417 in/on *Arabidopsis* roots and leaves 5 minutes, 1 hour (h), and 1 day (d) post-inoculation (pi) of plant roots with WCS417 by root-dip treatment. Brown bars indicate bacterial titres in/on the roots, green bars indicate bacterial titres in/on the leaves. The height of the bars represents the mean ± SE of two biologically independent experiments, including three replicates each. **(B)** Growth of bacteria in *A. thaliana* leaves. Leaves of 4-5-week-old *A. thaliana* plants were syringe-infiltrated with *Pseudomonas syringae* pathovar *tomato* (*Pst*) containing the effector *AvrRpm1* (positive control, red bars) or WCS417 (green bars) as indicated above the panel. The resulting *in planta* titres of these bacteria were monitored 2 h after inoculation (0 dpi) and six days later (6 dpi). Bars represent the mean of two biologically independent experiments, including three replicates each ± SE.

grown seedlings were treated with WCS417 or with sterile 10 mM $MgCl_2$ as a negative control and transferred to soil. 24 d later, leaves of the resulting plants were inoculated with *Pst*, *in planta* titres of which were determined at 4 dpi. Root-dip inoculation with WCS417 reduced the growth of the *Pst* inoculum in the leaves as compared to that in control plants (Figure 2A). Because WCS417 did not appear to directly inhibit *Pst* growth in a plate-based interaction assay (Figure S3A), the data suggest that treatment of *Arabidopsis* roots and associated propagation of WCS417 in the *Arabidopsis* phyllosphere triggers local IR against *Pst*.

Next, we sought to confirm that WCS417-triggered local IR was mediated by the plant immune system. In contrast to SAR, which is classically associated with SA signalling, WCS417-triggered systemic IR has previously been associated with JA signalling as well as an SA-independent function of NPR1 (Pieterse et al., 1996; Pieterse et al., 1998; Spoel et al., 2003; Pozo et al., 2008; Pieterse et al., 2021). *VEGETATIVE STORAGE PROTEIN 1* (*VSP1*) is a marker gene of the JA signalling pathway (Creelman & Mullet, 1997; Guerineau et al., 2003). Here, we tested whether local IR induction leads to changes in JA signalling by conducting an RT-qPCR analysis of *VSP1* transcript

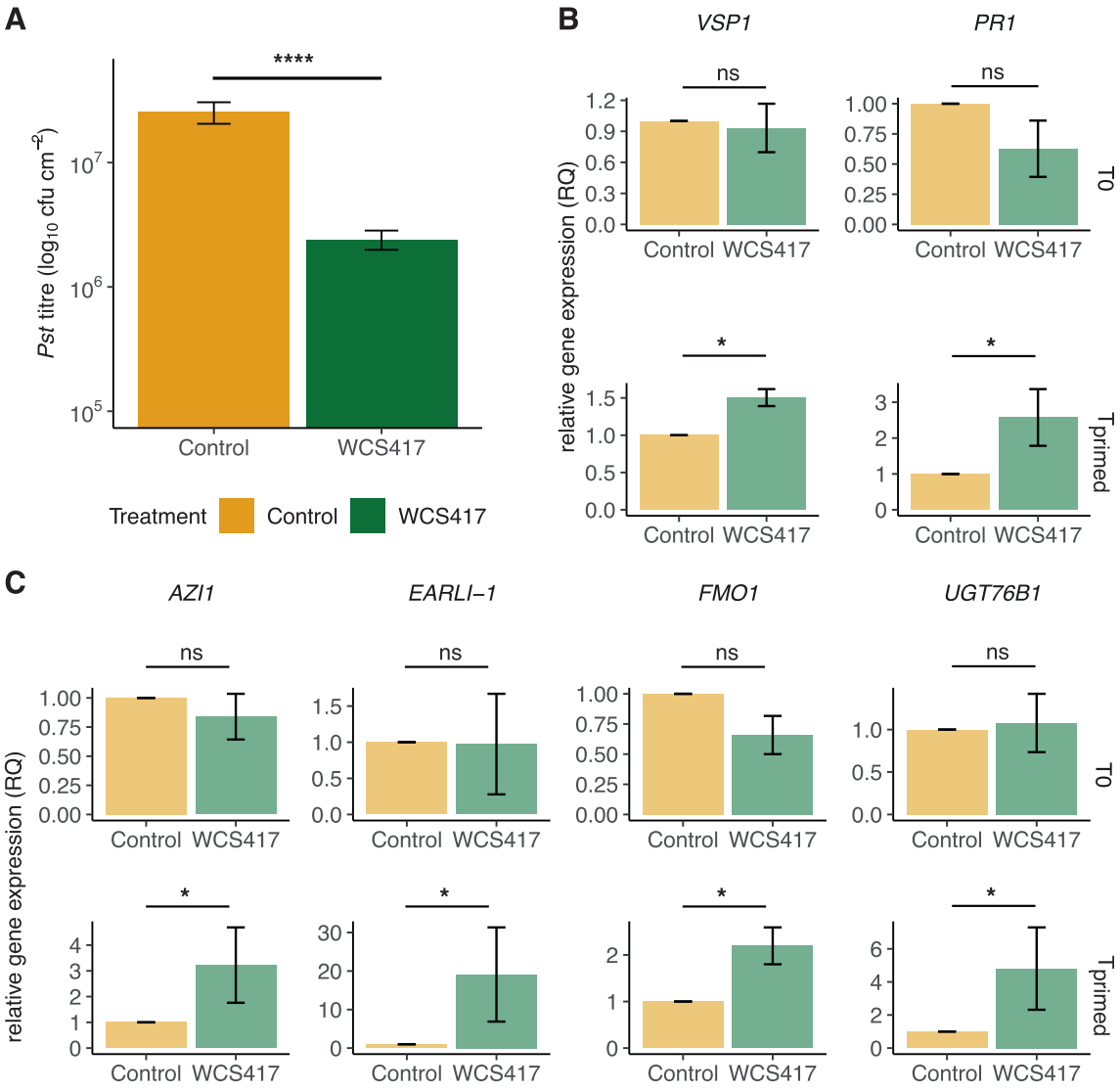

FIGURE 2 WCS417 triggers local induced resistance (IR) in *Arabidopsis* with priming of the JA, SA, and SAR marker genes *VSP1*, *PR1*, *AZI1*, *EARLI-1*, *FMO1*, and *UGT76B1*. The roots of 10-day-old, sterile-grown *A. thaliana* seedlings were inoculated with WCS417 (green bars) or a corresponding control solution (yellow bars). Following 3.5 weeks on soil, the leaves of the treated plants were infiltrated with *Pst*. **(A)** *In planta* *Pst* titres at 4 dpi. Bars represent the mean of three biologically independent experiments, including three replicates each ± SE. Asterisks indicate significant differences between the treatments indicated by the corresponding lines (Kruskal-Wallis test, ****, $p < 0.0001$; ns, not significantly different). **(B/C)** Transcript accumulation of *VSP1* and *PR1* **(B)** and of *AZI1*, *EARLI-1*, *FMO1*, *and UGT76B1* **(C)**. Transcript accumulation was evaluated by RT-qPCR in leaves of plants treated as in (A) and sampled before (T_0) or after infection (T_{primed}). T_{primed} indicates a merged analysis of maximum RQ-values per biologically independent experiment at 2, 4, and 6 hpi (Supplementary Figure S4). Transcript accumulation was normalized to that of *UBIQUITIN*. Bars represent mean values of three biologically independent experiments ± SE. Statistically significant differences were evaluated using a Kruskal-Wallis test, *, $p < 0.05$.

accumulation. Additionally, we tested a possible influence of local IR on SA signalling targeting the SA marker gene *PATHOGENESIS RELATED 1* (*PR1*) (van Loon et al., 2006) and on the SAR-associated genes *AZI1* and *EARLI1* (Jung et al., 2009; Yu et al., 2013; Cecchini et al., 2015) as well as *FMO1* and *UGT76B1*.

For the analysis of gene expression changes induced during local IR, leaves of WCS417- and control-treated plants were sampled before the challenge infection; these samples were designated as T_0. At this time point, the transcript levels of all tested genes were comparable in WCS417- and control-treated plants (Figure 2B/C). Often, full defence responses are not directly/constitutively activated after induction of IR. Rather, priming of defence responses leads to a stronger and faster response after a pathogenic challenge as compared to unprimed plants, which also culminates in enhanced resistance (Conrath et al., 2015; Martinez-Medina et al., 2016; Mauch-Mani et al., 2017). Because WCS417-triggered systemic IR is executed as a form of priming (Verhagen et al., 2004; Pieterse et al., 2014), we assessed primed gene expression changes during local IR at two, four, and six h post-inoculation (hpi) of the treated plants with *Pst*. Priming was detected in multiple biologically independent experiments but did not always peak at the same time point after inoculation (Figure S4). For this reason, we analysed the priming peaks per experiment in a merged analysis of T_{primed}. In this analysis, WCS417-treated plants displayed a significantly higher transcript level than control-treated plants of all tested genes (Figure 2B/C), confirming a priming effect of local IR on the transcript accumulation of *VSP1*, *PR1*, *AZI1*, *EARLI1*, *FMO1*, and *UGT76B1*. Thus, the data suggest that WCS417-triggered local IR is associated with priming of JA, SA, and SAR-associated gene expression changes.

3.3 | WCS417-triggered local IR depends on SA- and SAR-associated components of the plant immune system

WCS417-triggered systemic IR has been shown to depend on functional JA defences, but not on the accumulation of SA (Pieterse et al., 1996; Pieterse et al., 1998; Pozo et al., 2008). Here, we investigated WCS417-triggered local IR in *Arabidopsis* mutants with compromised MYC2-dependent JA defences (*jin1/myc2*) and also in mutants with compromised SA accumulation (*sid2-1*) and signalling (*npr1-1*) (Berger et al., 1996; Cao et al., 1997; Wildermuth et al., 2001; Pozo et al., 2008). Local IR was induced as described above, and the leaves of the plants were inoculated with *Pst*. Col-0 wild type supported less *Pst* growth in the leaves of plants pre-treated with WCS417 as compared to the controls, confirming that local IR was induced (Figure 3A/B). As reported before (Nickstadt et al., 2004), the *jin1* (*myc2*) mutant supported less *Pst* growth than Col-0 wild type plants. The absolute titres of *Pst* in control-treated *jin1*-plants were similar to those of wild type plants with functional WCS417-triggered local IR (Figure 3A). Similar to systemic IR (Pozo et al., 2008), WCS417-triggered local IR did not further lower bacterial titres in *jin1* mutant plants (Figure 3A). In contrast to systemic IR, however, WCS417-triggered local IR was ineffective and even appeared to enhance *Pst* growth slightly and significantly in *sid2-1* mutant plants. WCS417-triggered local IR was further dependent on functional NPR1 (Figure 3A). Together, the data suggest that WCS417-triggered local IR depended on MYC2 as well as on functional pathogen-induced SA accumulation and signalling.

Recent evidence further suggests roles of SAR-associated signalling intermediates in systemic IR (Cecchini et al., 2015; Shine et al., 2019). Here, we assessed the involvement of Pip-dependent pathways in local IR by using *ald1* mutant plants with defects in Pip biosynthesis (Návarová et al., 2012). We also tested the involvement of SAR-associated volatile monoterpenes by monitoring local IR in the respective loss-of-function mutant *ggpps12* (Riedlmeier et al., 2017; Wenig et al., 2019). In comparison to the respective control treatments, WCS417 did not reduce the growth of the *Pst* challenge inoculum in *ald1* and *ggpps12* plants, indicating that Pip and monoterpenes are essential in the realisation of immunity during WCS417-triggered local IR (Figure 3B). Taken together, the data suggest that WCS417-triggered local IR is dependent on SA, Pip, and monoterpenes, and might be triggered via a mechanism that is at least partially overlapping with SAR.

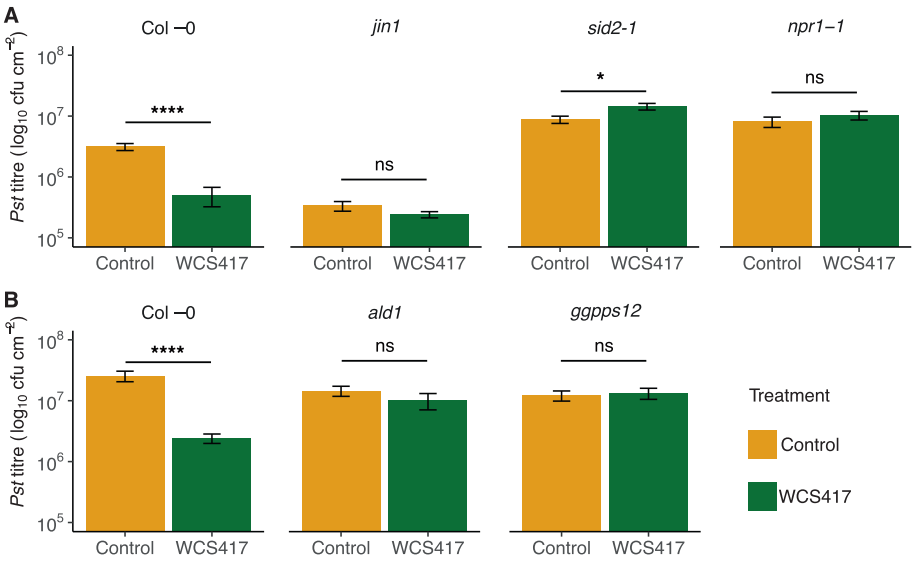

FIGURE 3 Characterization of the molecular requirements of WCS417-triggered local IR. The roots of 10-day-old seedlings of the genotypes indicated above the panels were inoculated with WCS417 (green bars) or a corresponding control solution (yellow bars). Following 3.5 weeks on soil, the leaves of the plants were inoculated with *Pst*. The resulting *in planta Pst* titres at 4 dpi are shown. Bars represent the mean of three biologically independent experiments with three replicates each ± SE. Asterisks indicate significant differences between the treatments indicated by the corresponding lines (Kruskal-Wallis test *, $p < 0.05$, **, $p < 0.01$, ***, $p < 0.001$, ****, $p < 0.0001$; ns, not significantly different).

3.4 | WCS417-triggered local IR changes the microbial composition of the phyllosphere

Defects in plant immunity have been shown to switch the role of certain bacteria from beneficial to pathogenic (Pfeilmeier et al., 2021). Chen et al. (2020) further illustrated a strong connection between plant immunity, the leaf microbiome, and plant health (Chen et al., 2020). Also, the PGPR *Bacillus velezensis* has been shown to enhance immunity in *Nicotiana tabacum* leaves by changing the phyllosphere microbiome (Liu et al., 2022). These findings emphasise the importance of the plant immune status for the leaf microbiome and *vice versa* and raise the question of whether induced resistance influences the leaf microbiome.

To address this question, we performed amplicon sequencing of the bacterial 16S rRNA gene in leaf samples from WCS417- and control-treated plants. Bacterial communities of WCS417-treated plants, on average, contained 165 different ASVs per sample in comparison to 361 different ASVs per sample in control-treated plants (Figure 4A and Figure S1). For this reason, we analysed ASV richness and evenness utilizing the Shannon's Index (Spellerberg & Fedor, 2003) and species richness as well as the dominance of single ASVs using the Simpson's Index (SIMPSON, 1949). The apparent lower species richness in WCS417-treated plants was confirmed by the Shannon's Index as well as the Simpson's index, which were both significantly lower in WCS417-treated than in control-treated plants (Figure 4A). Next, we assessed the similarity or divergence of the microbial composition of the different samples with regard to the abundance of the different ASVs using a principal component analysis (PCA). The PCA showed that the microbiome of plants treated with WCS417 clustered distinctly from that of control-treated plants (Figure 4B). Subsequently, we performed a MANOVA based on the distance matrix of the PCA to test for significant differences between the microbial composition following the different treatments. The phyllosphere microbiome of plants treated with WCS417 was significantly different from the phyllosphere microbiome of control plants. The treatment describes 38% of the differences between the treatments ($R^2 = 0.383$).

After this first explorative analysis of the data, we checked for the occurrence of WCS417 on the leaves of the plants. Therefore, we examined the absolute numbers of ASV3, whose 16S rRNA gene sequence corresponded to that of WCS417. In WCS417-treated plants, the reads of ASV3 on the leaves made up ~25% of the reads per sample (Figure 4C). This confirms the findings described above that root-dip inoculation of *Arabidopsis* results in the uptake and propagation of WCS417 in the plants' phyllosphere. ASV3 was not detected in the microbiome of control-treated plants, excluding cross-contamination between treatments during the local IR treatment.

13 different ASVs were present in all samples, of those, 12 stem from the phylum of Proteobacteria and one from the phylum of Actinobacteria. Concerning significant differences in the abundance of ASVs, WCS417-treated plants displayed a differential abundance of 6 ASVs in comparison to control-treated plants (Table S3). Most of the differentially accumulating ASVs were less abundant in local IR-treated compared to control-treated plants. Also, most of the significantly different ASVs were detected at relatively low read count numbers of <1% of all reads. Those ASVs comprise bacteria from the genera *Rhodopseudomonas*, *Rhodanobacter*, and *Acidothermus* as well as one bacterium from the Order Solirubrobacterales (Figure 4C). In contrast, one ASV besides the putative WCS417 (ASV3) was considerably enriched in the local IR-treated plants. In four out of five samples from WCS417-treated plants, an ASV linked to *Flavobacterium sp*. was detected at an average of 28% of all reads per sample, ranging from 3.5 to 39% (Figure 4C). By comparison, the same ASV was detected with 1 read in 1 control sample, and thus remained negligible on control-treated plants (Figure 4C). Thus, treatment of *Arabidopsis* with WCS417 was associated with significant enrichment of the phyllosphere microbiome with *Flavobacterium* sp..

3.5 | *Flavobacterium* sp. Leaf82 induces Systemic Acquired Resistance (SAR) in *Arabidopsis*

Since WCS417 proliferated in *Arabidopsis* leaves, we tested if this proliferation was causative for local IR. To this end, we infiltrated leaves of 4-5-week-old *Arabidopsis* plants with WCS417 or with 10 mM $MgCl_2$ as the negative control. Two days later, we performed a challenge inoculation of the same leaves with *Pst*. As expected, WCS417 treatment of the leaves caused a reduction of *Pst* proliferation as compared to the control (Figure 5A), confirming that leaf-associated WCS417 was at least partially responsible for triggering local IR in *Arabidopsis*. Similarly to a root-dip inoculation, leaf infiltration with WCS417 did not enhance the resistance of *npr1-1* plants to *Pst* (Figure 5A).

The relative abundance of *Flavobacterium* sp. (ASV4) was significantly enhanced on the leaves of WCS417-treated plants (Figure 4C). To study a possible new plant immunity-related interaction between the plant and the phyllosphere, we next aimed to test if this bacterium affects defence. As a proxy for *Flavobacterium* sp., we utilized a bacterial strain, Leaf82, from the *At*-LSPHERE collection (Bai et al., 2015), which displays 100% sequence identity of its V5-V7 16S rRNA gene region with that of ASV4. First, Leaf82 was syringe-infiltrated into leaves of 4-5-week-old *Arabidopsis* plants. Two days later, the same leaves were infiltrated with *Pst*. In contrast to WCS417, local Leaf82 treatment did not reduce *Pst* proliferation on the leaves and thus did not induce local IR (Figure 5B).

To evaluate whether the proliferation of Leaf82 might affect plant resistance systemically, we infiltrated the first and second true leaves of either wild type or *npr1-1* mutant *Arabidopsis* plants with Leaf82 and challenged the systemic leaves with *Pst*. As a positive control, we used *Pst/AvrRpm1* for the primary treatment; as a negative control, the plants were infiltrated with 10 mM $MgCl_2$. In wild type plants, *Pst* proliferation was reduced in the systemic tissue of plants undergoing a local *Pst/AvrRpm1* infection as compared to the negative control, indicating a successful SAR response (Figure 5C). Similarly, a local Leaf82 treatment reduced the propagation of a systemic *Pst* inoculum as compared to the negative control treatment, suggesting

the induction of SAR in response to Leaf82 (Figure 5C). In *npr1* mutant plants, *Pst* titres were similar irrespective of the treatment, suggesting that Leaf82-induced SAR was abolished in the absence of functional NPR1 (Figure 5C). Thus, Leaf82 triggers SAR against *Pst* and this response is dependent on *NPR1*.

3.6 | Microbe-microbe-host interactions in the *Arabidopsis* phyllosphere

Finally, we investigated whether local WCS417-induced defence responses of *Arabidopsis* influenced the proliferation of *Flavobacterium*

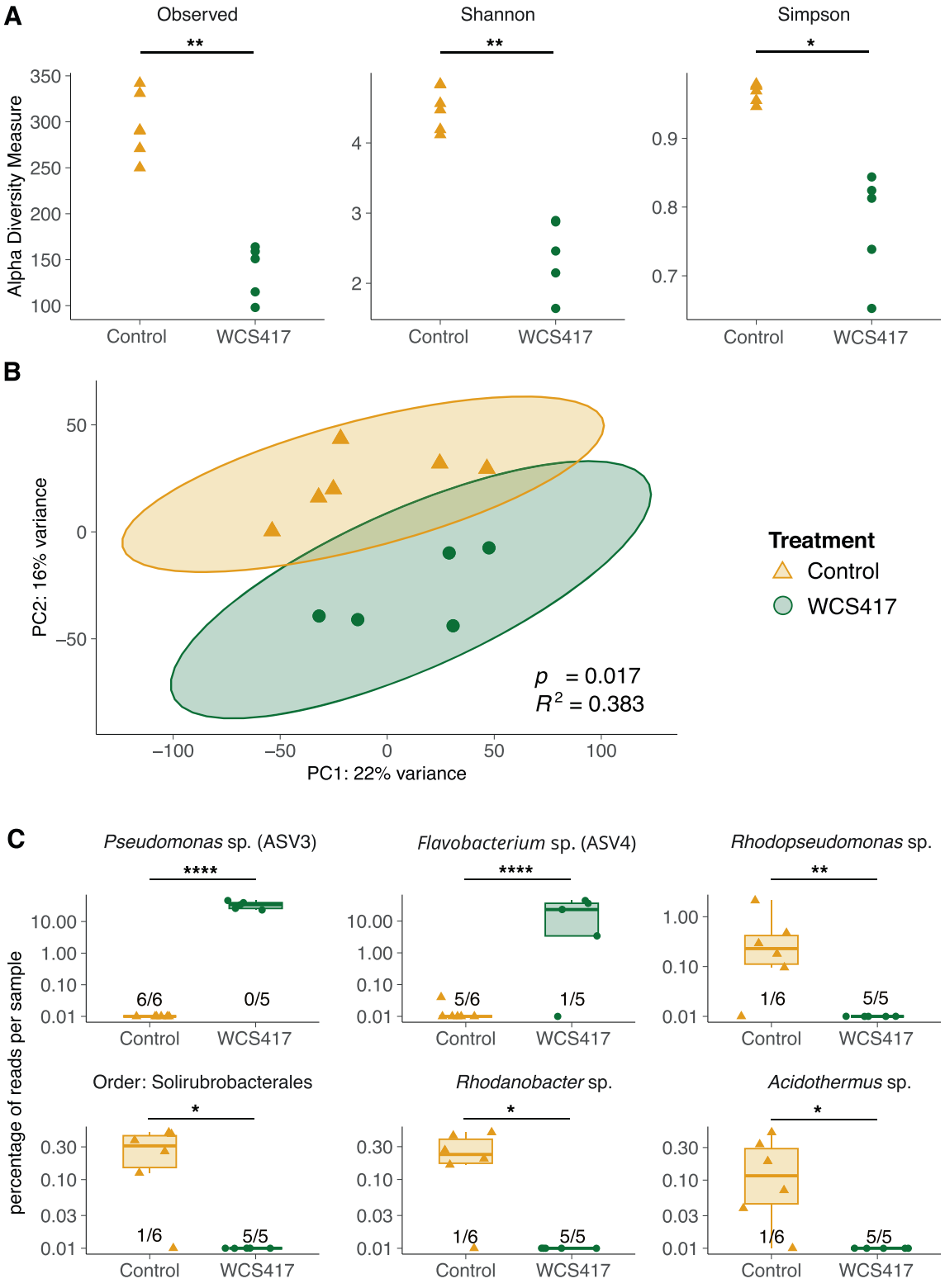

FIGURE 4 Legend on next page.

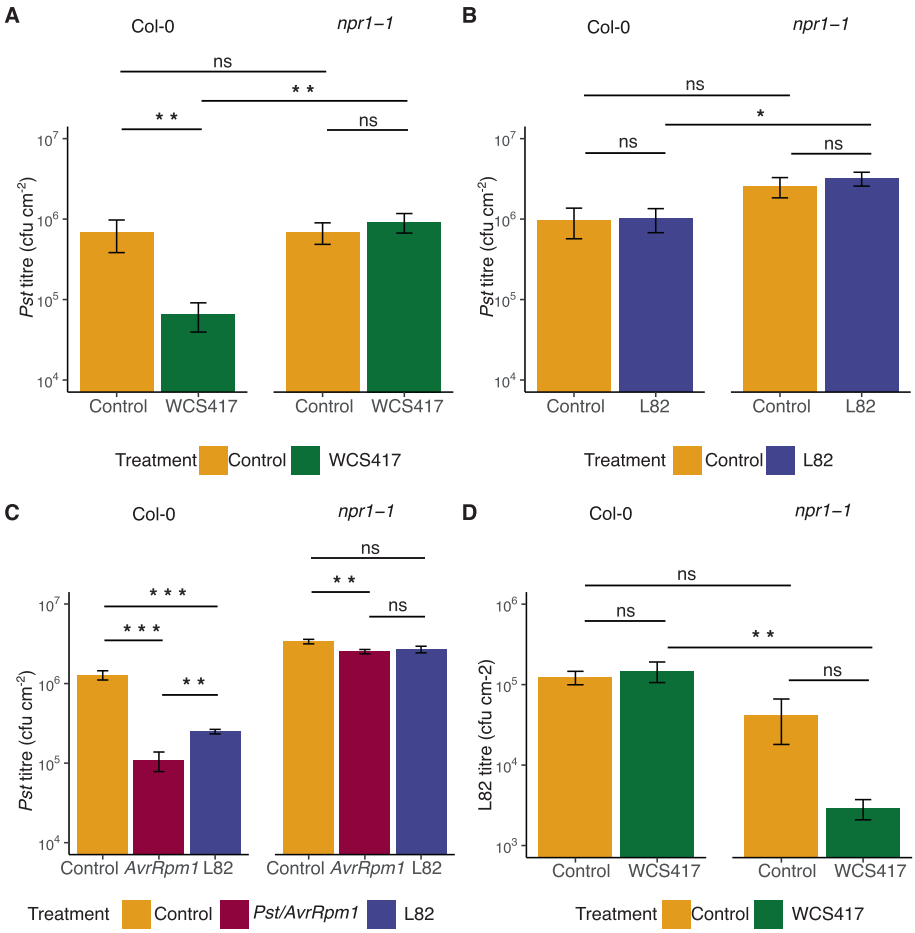

FIGURE 5 Local and systemic plant-microbe-microbe interactions. Leaves of 4–5 week old Col-0 wild type and *npr1-1* mutant *Arabidopsis* plants (genotypes indicated above the panels) were infiltrated with WCS417 (green bars in **A/D**), *At*-L-Sphere *Flavobacterium sp.* Leaf82 (L82; purple bars in **B/C**), or a corresponding negative control solution (yellow bars in **A-C**) or with *Pst/AvrRpm1* as a positive control (red bars in **C**). Two days later, the same leaves were infiltrated with *Pst* **(A/B)** or Leaf82 **(D)** or two systemic leaves were infiltrated with *Pst* **(C),** titres of which were determined at 4 dpi. Bars represent average *in planta Pst* **(A/B/C)** and Leaf82 **(D)** titres from 6 to 9 samples derived from two **(D)** to three biologically independent experiments **(A/B/C)** ± SE. Asterisks indicate significant differences between the treatments indicated by the corresponding lines (**A/B/D**: Kruskal-Wallis test, **C**: paired samples Wilcoxon test, *, $p < 0.05$, **, $p < 0.01$, ***, $p < 0.001$; ns, not significantly different).

sp. during local IR. To this end, we performed the same experiment as above and infiltrated leaves of 4-5-week-old *Arabidopsis* plants with WCS417 or with 10 mM $MgCl_2$ as the negative control. Two days later, we infiltrated the same leaves with Leaf82. Although WCS417-triggered local IR was associated with enhanced proliferation of *Flavobacterium sp.* on the leaves, leaf inoculation of WCS417 did not cause enhanced growth of a subsequent Leaf82 inoculum (Figure 5D). In contrast, the proliferation of Leaf82 was reduced on WCS417-treated *npr1* mutants as compared to the wild type control (Figure 5D). Similarly, WCS417 proliferated less on *npr1* mutant than on wild type plants (Figure S5). Thus, the data suggest that WCS417 activates *NPR1*-dependent responses in plants that reduce the growth of pathogenic *Pst* and, at the same time, enhance WCS417 proliferation. Because Leaf82 titres did not appear to be directly regulated by local WCS417 proliferation (Figure 5D and Figure S3B) but were reduced on *npr1* mutant plants in the presence of WCS417 (Figure 5D and Figure S5), the data suggest that *Flavobacterium* sp. is subject to immunity-related plant-microbe-microbe interactions in the phyllosphere.

FIGURE 4 Differences in the microbiome of the phyllosphere following WCS417 IR treatment in comparison to control-treated plants. Leaves of plants grown for 3.5 weeks on soil after root-dip inoculation with either 10 mM $MgCl_2$ (control treatment, yellow triangles) or WCS417 (green dots) were harvested and amplicon sequencing of the 16S rRNA gene was performed. **(A)** Principal Component Analysis of the overall microbial composition, PC1 and PC2 represent the respective principal components with the corresponding explained variance in percent. The *p*-value was calculated using a MANOVA based on the Euclidian distance matrix of the PCA and was corrected for multiple testing using the Benjamini-Hochberg procedure. The effect size describes the percentage of variance explained by treatment. **(B)** α-diversity indices of phyllosphere microbiome following WCS417- or control-treatment: Number of observed ASVs (left) Shannon's Index (middle) and Simpson's Index (right). The y-axis represents the respective index value, and dots indicate the values of individual samples. Samples from WCS417-treated plants have significantly lower ASV-numbers as well as α-diversity indices than control-treated plants (pairwise pat-test, *, $p < 0.05$, **, $p < 0.01$). **(C)** Relative abundance of distinct bacterial species in the *A. thaliana* phyllosphere. Boxplots indicate average number of sequenced reads corresponding to the species indicated above the panels from five (WCS417) to six (control) samples in percentage of reads per sample ± min and max values. Numbers at the bottom of the boxplots indicate number of samples with zero read counts per species / total number of samples. Significance was calculated using a built-in Wald-test of the DESeq2-package with FDR correction following the Benjamini-Hochberg procedure *, $p < 0.05$, **, $p < 0.01$, ****, $p < 0.0001$.

4 | DISCUSSION

We could prove in this work that leaf-associated *P. simiae* WCS417r triggers SA-dependent local IR against *Pst* in *Arabidopsis* (Figure 3). Additionally, WCS417-triggered local IR was not observed in plants which lacked functional MYC2, the master regulator of JA signalling (Kazan & Manners, 2013). Whereas the latter is reminiscent of systemic IR in response to treatment of soil with WCS417 (Pozo et al., 2008), priming of *VSP1* appeared moderate in comparison to that of the SA marker gene *PR1* and the SAR-associated genes *AZI1*, *EARLI1*, *FMO1*, and *UGT76B1* (Figure 2 and Supplementary Figure S4). Also, while WCS417-triggered systemic IR was functional in SA-deficient *NahG* plants (Pieterse et al., 1996), WCS417-triggered local IR was abolished in both *sid2* and *npr1* mutant plants (Figure 3). These data support previous findings that different mechanisms of IR can occur in response to different plant-microbe interactions (reviewed in (Gill et al., 2016; Pieterse et al., 2021; Vlot et al., 2021; Khan et al., 2023). Differences may depend on the specific PGPR and challenge pathogen involved (Ton et al., 2002; van de Mortel et al., 2012; Nguyen et al., 2020; Nguyen et al., 2022). We show here that the same PGPR can prime different phytohormone signalling pathways depending on the site of the plant-microbe interactions involved. WCS417-triggered local IR neither conforms to the traditional definition of ISR, which refers to systemic IR in response to a root interaction with beneficial microbes (Pieterse et al., 2014), nor to that of SAR, which refers to systemic IR in response to a leaf interaction with a pathogen (Vlot et al., 2021). Thus, our data support suggestions made by De Kesel and colleagues (Kesel et al., 2021) that the distinction between ISR and SAR is blurring and that terminology such as local versus systemic IR might be more appropriate to conceptualize IR across different plant-microbe interaction systems. Therefore, we used the terms WCS417-triggered local and systemic IR throughout this work to differentiate between two modes of IR triggered by the same PGPR. Whereas WCS417-triggered systemic IR is associated with JA signalling (Pieterse et al., 1998; Ton et al., 2002; Pozo et al., 2008), local IR additionally depends on functional SA biosynthesis and signalling (this work). Our finding that WCS417 can reach the phyllosphere in root-dip assays may be of interest to other studies using similar methods, including multi-well assays.

In addition to SA, WCS417-triggered local IR depends on further signalling intermediates that are associated with classical SAR (Figure 3). These include functional Pip biosynthesis and the accumulation of volatile monoterpenes, which occur downstream of Pip during SAR (Návarová et al., 2012; Riedlmeier et al., 2017; Wenig et al., 2019). Systemic IR often depends on priming, which means that the plant does not directly increase its gene expression upon contact with PGPR. Instead, there are more subtle, often epigenetic changes, which lead to a faster and stronger response after contact with pathogens in comparison to naïve plants without previous contact with PGPR (Conrath et al., 2015; Martinez-Medina et al., 2016; Mauch-Mani et al., 2017; Kesel et al., 2021). For WCS417-triggered systemic IR, this phenomenon has been described (van Wees et al., 1999; Pieterse et al., 2021). Here, we extended these findings to WCS417-triggered local IR and showed priming of *AZI1*, *EARLI*, *FMO1*, *PR1*, *VSP1*, and *UGT761B* in response to WCS417, preparing the plants for a more effective immune response after infection. Of these genes, *AZI1*, *EARLI1*, and *FMO1* are part of the Pip-dependent signalling pathway that promotes SAR in parallel with SA (Jung et al., 2009; Wang et al., 2014; Cecchini et al., 2015; Chen et al., 2018; Hartmann et al., 2018; Wang et al., 2018; Wenig et al., 2019). Taken together, the data suggest that WCS417 triggers local IR in *Arabidopsis* leaves; WCS417-triggered local IR depends on both JA and SA signalling in a mechanism which partially overlaps with systemic IR in response to WCS417 and with classical SAR.

The plant immune system is believed to influence plant-associated microbiota (Hacquard et al., 2017; Teixeira et al., 2019; Stassen et al., 2021; Sohrabi et al., 2023). Here, WCS417-triggered local IR was associated with a higher relative abundance of *Flavobacterium sp*. in the *Arabidopsis* phyllosphere. Concomitantly, the phyllosphere microbiome of WCS417-treated plants displayed a significantly reduced species richness. Because lower richness in microbiota has been associated with a lower stability of the microbiome and a higher risk of dominance by pathogens (Ives & Hughes, 2002; Chen et al., 2020; Chaudhry et al., 2021), this suggests a possible trade-off of IR in plants. In this respect, it seems of interest that we detected considerably less significant shifts in the phyllosphere microbiome composition than Chen et al. (2020), who studied the influence of local immune responses driven by pathogen-associated molecular patterns (PAMPs) on the phyllosphere microbiome. The comparatively moderate phyllosphere microbiome changes in response to IR likely reflect the fact that WCS417-triggered local IR is primed. Thus, there are only minor changes in gene expression up to the point of pathogenic encounter. This is in contrast to the experimental set-up of Chen et al., who analysed the microbiome of a quadruple knockout, which shows defects in PAMP-triggered immunity (PTI). The ensuing changes in gene expression compared to wild-type plants lead to more significant shifts in the relative abundance of Proteobacteria (up) and Actinobacteria (down) (Chen et al., 2020). Deployment of this "incorrectly" assembled microbiome onto gnotobiotic plants led to necrosis and stunted plant growth. These findings associate compromised PTI responses with reduced plant fitness caused by changes in the phyllosphere microbiome, whereas priming appears to have a significantly less pronounced effect.

Propagation of WCS417 in the phyllosphere appears to be actively regulated by NPR1-mediated plant immunity. Data shown in Figure 5, as well as Figure S5, further suggest a possible co-regulation of WCS417 and Leaf82 in interaction with the plant immune regulator NPR1. Notably, Leaf82 growth was not directly influenced by WCS417 in plate-based interaction assays (Figure S3B). However, *Flavobacterium johnsoniae*, to which species Leaf82 belongs, has been shown to adapt production of secondary metabolites if grown in association with a *Pseudomonas koreensis* and a *Bacillus cereus* strain, facilitating better chances of surface colonisation and biofilm formation (Chevrette et al., 2022). Thus, it is conceivable that improved colonization of *Flavobacterium* sp. on WCS417-treated plants depended on the tri-partite interaction between the plant and both microbes.

Species belonging to the genus *Flavobacterium* are known to be well-adapted to the phyllosphere, living epi- as well as endophytically on *Arabidopsis* plants (Bodenhausen et al., 2013). They can metabolize

complex carbon sources, including pectin, hemicellulose, and peptidoglycan components of gram-positive cell walls of bacteria (Peterson et al., 2006; Kolton et al., 2013). By those attributes, *Flavobacteria* spp. can outcompete other bacterial groups. Additionally, they have been assigned enhanced biocontrol as well as plant growth-promoting properties. *Flavobacterium* spp., for example, produces cyanide acting as an antimicrobial agent as well as compounds that act as plant growth-promoting hormones, including auxins, gibberellins and cytokinins (Gunasinghe et al., 2004; Maimaiti et al., 2007; Soltani et al., 2010; Sang & Kim, 2012). Indeed, we observed enhanced growth of *Arabidopsis* plants after inoculation of the leaves with *At*-LSPHERE *Flavobacterium sp*. Leaf82 (Figure S6). Leaf82 also triggered NPR1-dependent SAR, thus additionally heightening plant resistance (Figure 5). Because Leaf82 did not appear to restrict *Pst* growth in plate-based interaction assays (Figure S3C), leaf82-induced SAR is likely a plant immunity-mediated process. Vogel et al. (2021) ascribed only moderate biocontrol properties to Leaf82 against *Pst* in gnotobiotic experiments with *Arabidopsis*. However, they found strong evidence that the protective traits of bacteria shift strongly in association with other bacterial strains (Vogel et al., 2021). Thus, Leaf 82 might unfold its full protective potential only in the presence of other bacteria in the leaf microbiome.

In conclusion, WCS417-triggered local IR is associated with the enrichment of the *Arabidopsis* phyllosphere with *Flavobacterium sp. Flavobacterium* Leaf82 was identified to display beneficial characteristics triggering NPR1-dependent systemic IR in *Arabidopsis*. This paves the way for further studies into possible applications of this bacterium in new, sustainable crop protection strategies.

AUTHOR CONTRIBUTIONS

MS and ACV conceived the project; AS, MW, SK, BUF, and ACV planned experiments, AS, MW, CK, and SK executed experiments, AS, MW, CK, SK, BUF, and ACV analysed the data, AS and ACV wrote the manuscript, MS edited the manuscript, all authors read and commented on the manuscript.

ACKNOWLEDGEMENTS

The authors thank Carina Heuschmann and Eva Möller (University of Bayreuth, Germany) for technical assistance, Dr. Corné M.J. Pieterse (Utrecht University, The Netherlands) for sharing *Pseudomonas simiae* WCS417r, and Dr. Julia Vorholt (ETH Zürich, Switzerland) for providing *At*-LSPHERE Leaf82 and for helpful advice on this work. This work was funded by the DFG as part of the priority program SPP 2125 (to MS and ACV). Open Access funding enabled and organized by Projekt DEAL.

FUNDING INFORMATION

This work was funded by the DFG as part of the priority program SPP 2125 (to MS and ACV).

DATA AVAILABILITY STATEMENT

The data that support the findings of this study are openly available in the NCBI Sequence Read Archive at https://www.ncbi.nlm.nih.gov/bioproject/PRJNA1127464/, reference number PRJNA1127464. All further data are available from the corresponding author upon reasonable request.

ORCID

A. Corina Vlot https://orcid.org/0000-0002-8146-6018

REFERENCES

Bai, Y., Müller, D.B., Srinivas, G., Garrido-Oter, R., Potthoff, E. & Rott, M. et al. (2015) Functional overlap of the Arabidopsis leaf and root microbiota. *Nature*, 528(7582), 364–369.

Bauer, S., Mekonnen, D.W., Hartmann, M., Yildiz, I., Janowski, R. & Lange, B. et al. (2021) UGT76B1, a promiscuous hub of small molecule-based immune signaling, glucosylates N-hydroxypipecolic acid, and balances plant immunity. *The Plant Cell*, 33(3), 714–734.

Berendsen, R.L., Vismans, G., Yu, K., Song, Y., de Jonge, R. & Burgman, W.P. et al. (2018) Disease-induced assemblage of a plant-beneficial bacterial consortium. *The ISME Journal*, 12(6), 1496–1507.

Berger, S., Bell, E. & Mullet, J.E. (1996) Two Methyl Jasmonate-Insensitive Mutants Show Altered Expression of AtVsp in Response to Methyl Jasmonate and Wounding. *Plant Physiology*, 111(2), 525–531.

Bodenhausen, N., Horton, M.W. & Bergelson, J. (2013) Bacterial communities associated with the leaves and the roots of Arabidopsis thaliana. *PloS One*, 8(2), e56329.

Breitenbach, H.H., Wenig, M., Wittek, F., Jordá, L., Maldonado-Alconada, A.M. & Sarioglu, H. et al. (2014) Contrasting Roles of the Apoplastic Aspartyl Protease APOPLASTIC, ENHANCED DISEASE SUSCEPTIBILITY1-DEPENDENT1 and LEGUME LECTIN-LIKE PROTEIN1 in Arabidopsis Systemic Acquired Resistance. *Plant Physiology*, 165(2), 791–809.

Bulgarelli, D., Rott, M., Schlaeppi, K., Ver Loren Themaat, E., Ahmadinejad, N. & Assenza, F. et al. (2012) Revealing structure and assembly cues for Arabidopsis root-inhabiting bacterial microbiota. *Nature*, 488(7409), 91–95.

Cai, J., Jozwiak, A., Holoidovsky, L., Meijler, M.M., Meir, S. & Rogachev, I. et al. (2021) Glycosylation of N-hydroxy-pipecolic acid equilibrates between systemic acquired resistance response and plant growth. *Molecular Plant*, 14(3), 440–455.

Callahan, B.J., McMurdie, P.J., Rosen, M.J., Han, A.W., Johnson, A.J.A. & Holmes, S.P. (2016) DADA2: High-resolution sample inference from Illumina amplicon data. *Nature Methods*, 13(7), 581–583.

Cao, H., Glazebrook, J., Clarke, J.D., Volko, S. & Dong, X. (1997) The Arabidopsis NPR1 gene that controls systemic acquired resistance encodes a novel protein containing ankyrin repeats. *Cell*, 88(1), 57–63.

Cecchini, N.M., Steffes, K., Schläppi, M.R., Gifford, A.N. & Greenberg, J.T. (2015) Arabidopsis AZI1 family proteins mediate signal mobilization for systemic defence priming. *Nature Communications*, 6, 7658.

Chanda, B., Xia, Y., Mandal, M.K., Yu, K., Sekine, K.-T. & Gao, Q.-M. et al. (2011) Glycerol-3-phosphate is a critical mobile inducer of systemic immunity in plants. *Nature Genetics*, 43(5), 421–427.

Chaudhry, V., Runge, P., Sengupta, P., Doehlemann, G., Parker, J.E. & Kemen, E. (2021) Shaping the leaf microbiota: plant-microbe-microbe interactions. *Journal of Experimental Botany*, 72(1), 36–56.

Chelius, M.K. & Triplett, E.W. (2001) The Diversity of Archaea and Bacteria in Association with the Roots of Zea mays L. *Microbial Ecology*, 41(3), 252–263.

Chen, L. & Liu, Y. (2024) The Function of Root Exudates in the Root Colonization by Beneficial Soil Rhizobacteria. *Biology*, 13(2).

Chen, T., Nomura, K., Wang, X., Sohrabi, R., Xu, J. & Yao, L. et al. (2020) A plant genetic network for preventing dysbiosis in the phyllosphere. *Nature*, 580(7805), 653–657.

Chen, Y.-C., Holmes, E.C., Rajniak, J., Kim, J.-G., Tang, S. & Fischer, C.R. et al. (2018) N-hydroxy-pipecolic acid is a mobile metabolite that

induces systemic disease resistance in Arabidopsis. *Proceedings of the National Academy of Sciences of the United States of America*, 115(21), E4920-E4929.

Chevrette, M.G., Thomas, C.S., Hurley, A., Rosario-Meléndez, N., Sankaran, K. & Tu, Y. et al. (2022) Microbiome composition modulates secondary metabolism in a multispecies bacterial community. *Proceedings of the National Academy of Sciences of the United States of America*, 119(42), e2212930119.

Conrath, U., Beckers, G.J.M., Langenbach, C.J.G. & Jaskiewicz, M.R. (2015) Priming for enhanced defense. *Annual Review of Phytopathology*, 53, 97–119.

Creelman, R.A. & Mullet, J.E. (1997) BIOSYNTHESIS AND ACTION OF JASMONATES IN PLANTS. *Annual Review of Plant Physiology and Plant Molecular Biology*, 48, 355–381.

Ding, P., Rekhter, D., Ding, Y., Feussner, K., Busta, L. & Haroth, S. et al. (2016) Characterization of a Pipecolic Acid Biosynthesis Pathway Required for Systemic Acquired Resistance. *The Plant Cell*, 28(10), 2603–2615.

Ding, Y., Sun, T., Ao, K., Peng, Y., Zhang, Y. & Li, X. et al. (2018) Opposite Roles of Salicylic Acid Receptors NPR1 and NPR3/NPR4 in Transcriptional Regulation of Plant Immunity. *Cell*, 173(6), 1454-1467.e15.

Dixon, P. (2003) VEGAN, a package of R functions for community ecology. *Journal of Vegetation Science*, 14(6), 927–930.

Eccleston, L., Brambilla, A. & Vlot, A.C. (2022) New molecules in plant defence against pathogens. *Essays in Biochemistry*, 66(5), 683–693.

Fu, Z.Q., Yan, S., Saleh, A., Wang, W., Ruble, J. & Oka, N. et al. (2012) NPR3 and NPR4 are receptors for the immune signal salicylic acid in plants. *Nature*, 486(7402), 228–232.

Gill, S.S., Gill, R., Trivedi, D.K., Anjum, N.A., Sharma, K.K. & Ansari, M.W. et al. (2016) Piriformospora indica: Potential and Significance in Plant Stress Tolerance. *Frontiers in Microbiology*, 7, 332.

Grubbs, F.E. (1950) Sample Criteria for Testing Outlying Observations. *The Annals of Mathematical Statistics*, 21(1), 27–58.

Guerineau, F., Benjdia, M. & Zhou, D.X. (2003) A jasmonate-responsive element within the A. thaliana vsp1 promoter. *Journal of Experimental Botany*, 54(385), 1153–1162.

Gunasinghe, R.N., Ikiriwatte, C.J. & Karunaratne, A.M. (2004) The use of Pantoea agglomerans and Flavobacterium sp. to control banana pathogens. *The Journal of Horticultural Science and Biotechnology*, 79(6), 1002–1006.

Hacquard, S., Spaepen, S., Garrido-Oter, R. & Schulze-Lefert, P. (2017) Interplay Between Innate Immunity and the Plant Microbiota. *Annual Review of Phytopathology*, 55, 565–589.

Hartmann, M., Kim, D., Bernsdorff, F., Ajami-Rashidi, Z., Scholten, N. & Schreiber, S. et al. (2017) Biochemical Principles and Functional Aspects of Pipecolic Acid Biosynthesis in Plant Immunity. *Plant Physiology*, 174(1), 124–153.

Hartmann, M. & Zeier, J. (2019) N-hydroxypipecolic acid and salicylic acid: a metabolic duo for systemic acquired resistance. *Current Opinion in Plant Biology*, 50, 44–57.

Hartmann, M., Zeier, T., Bernsdorff, F., Reichel-Deland, V., Kim, D. & Hohmann, M. et al. (2018) Flavin Monooxygenase-Generated N-Hydroxypipecolic Acid Is a Critical Element of Plant Systemic Immunity. *Cell*, 173(2), 456-469.e16.

Holmes, E.C., Chen, Y.-C., Mudgett, M.B. & Sattely, E.S. (2021) Arabidopsis UGT76B1 glycosylates N-hydroxy-pipecolic acid and inactivates systemic acquired resistance in tomato. *The Plant Cell*, 33(3), 750–765.

Ives, A.R. & Hughes, J.B. (2002) General relationships between species diversity and stability in competitive systems. *The American Naturalist*, 159(4), 388–395.

Jung, H.W., Tschaplinski, T.J., Wang, L., Glazebrook, J. & Greenberg, J.T. (2009) Priming in systemic plant immunity. *Science (New York, N.Y.)*, 324(5923), 89–91.

Kazan, K. & Manners, J.M. (2013) MYC2: the master in action. *Molecular Plant*, 6(3), 686–703.

de Kesel, J., Conrath, U., Flors, V., Luna, E., Mageroy, M.H. & Mauch-Mani, B. et al. (2021) The Induced Resistance Lexicon: Do's and Don'ts. *Trends in Plant Science*, 26(7), 685–691.

Khan, A.R., Mustafa, A., Hyder, S., Valipour, M., Rizvi, Z.F. & Gondal, A.S. et al. (2022) Bacillus spp. as Bioagents: Uses and Application for Sustainable Agriculture. *Biology*, 11(12).

Khan, R.A.A., Najeeb, S., Chen, J., Wang, R., Zhang, J. & Hou, J. et al. (2023) Insights into the molecular mechanism of Trichoderma stimulating plant growth and immunity against phytopathogens. *Physiologia Plantarum*, 175(6), e14133.

Kolton, M., Sela, N., Elad, Y. & Cytryn, E. (2013) Comparative genomic analysis indicates that niche adaptation of terrestrial Flavobacteria is strongly linked to plant glycan metabolism. *PloS One*, 8(9), e76704.

Kong, X., Zhang, C., Zheng, H., Sun, M., Zhang, F. & Zhang, M. et al. (2020) Antagonistic Interaction between Auxin and SA Signaling Pathways Regulates Bacterial Infection through Lateral Root in Arabidopsis. *Cell Reports*, 32(8), 108060.

Lim, G.-H., Shine, M.B., Lorenzo, L. de, Yu, K., Cui, W. & Navarre, D. et al. (2016) Plasmodesmata Localizing Proteins Regulate Transport and Signaling during Systemic Acquired Immunity in Plants. *Cell Host & Microbe*, 19(4), 541–549.

Liu, H., Jiang, J., An, M., Li, B., Xie, Y. & Xu, C. et al. (2022) Bacillus velezensis SYL-3 suppresses Alternaria alternata and tobacco mosaic virus infecting Nicotiana tabacum by regulating the phyllosphere microbial community. *Frontiers in Microbiology*, 13, 840318.

Liu, Y., Sun, T., Sun, Y., Zhang, Y., Radojičić, A. & Ding, Y. et al. (2020) Diverse Roles of the Salicylic Acid Receptors NPR1 and NPR3/NPR4 in Plant Immunity. *The Plant Cell*, 32(12), 4002–4016.

Love, M.I., Huber, W. & Anders, S. (2014) Moderated estimation of fold change and dispersion for RNA-seq data with DESeq2. *Genome Biology*, 15(12), 550.

Maimaiti, J., Zhang, Y., Yang, J., Cen, Y.-P., Layzell, D.B. & Peoples, M. et al. (2007) Isolation and characterization of hydrogen-oxidizing bacteria induced following exposure of soil to hydrogen gas and their impact on plant growth. *Environmental Microbiology*, 9(2), 435–444.

Martínez-Medina, A., Fernández, I., Sánchez-Guzmán, M.J., Jung, S.C., Pascual, J.A. & Pozo, M.J. (2013) Deciphering the hormonal signalling network behind the systemic resistance induced by Trichoderma harzianum in tomato. *Frontiers in Plant Science*, 4, 206.

Martinez-Medina, A., Flors, V., Heil, M., Mauch-Mani, B., Pieterse, C.M.J. & Pozo, M.J. et al. (2016) Recognizing Plant Defense Priming. *Trends in Plant Science*, 21(10), 818–822.

Mauch-Mani, B., Baccelli, I., Luna, E. & Flors, V. (2017) Defense Priming: An Adaptive Part of Induced Resistance. *Annual Review of Plant Biology*, 68, 485–512.

McMurdie, P.J. & Holmes, S. (2013) phyloseq: an R package for reproducible interactive analysis and graphics of microbiome census data. *PloS One*, 8(4), e61217.

McMurdie, P.J. & Holmes, S. (2014) Waste not, want not: why rarefying microbiome data is inadmissible. *PLoS Computational Biology*, 10(4), e1003531.

Misas-Villamil, J.C., Kolodziejek, I. & van der Hoorn, R.A.L. (2011) Pseudomonas syringae colonizes distant tissues in Nicotiana benthamiana through xylem vessels. *The Plant Journal*, 67(5), 774–782.

Mohnike, L., Rekhter, D., Huang, W., Feussner, K., Tian, H. & Herrfurth, C. et al. (2021) The glycosyltransferase UGT76B1 modulates N-hydroxy-pipecolic acid homeostasis and plant immunity. *The Plant Cell*, 33(3), 735–749.

Müller, D.B., Vogel, C., Bai, Y. & Vorholt, J.A. (2016) The Plant Microbiota: Systems-Level Insights and Perspectives. *Annual Review of Genetics*, 50, 211–234.

Nair, A., Goyal, I., Voß, E., Mrozek, P., Prajapati, S. & Thurow, C. et al. (2021) N-hydroxypipecolic acid-induced transcription requires the salicylic acid signaling pathway at basal SA levels. *Plant Physiology*, 187(4), 2803–2819.

Návarová, H., Bernsdorff, F., Döring, A.-C. & Zeier, J. (2012) Pipecolic acid, an endogenous mediator of defense amplification and priming, is a critical regulator of inducible plant immunity. *The Plant Cell*, 24(12), 5123–5141.

Newitt, J.T., Prudence, S.M.M., Hutchings, M.I. & Worsley, S.F. (2019) Biocontrol of Cereal Crop Diseases Using Streptomycetes. *Pathogens (Basel, Switzerland)*, 8(2).

Nguyen, N.H., Trotel-Aziz, P., Villaume, S., Rabenoelina, F., Clément, C. & Baillieul, F. et al. (2022) Priming of camalexin accumulation in induced systemic resistance by beneficial bacteria against Botrytis cinerea and Pseudomonas syringae pv. tomato DC3000. *Journal of Experimental Botany*, 73(11), 3743–3757.

Nguyen, N.H., Trotel-Aziz, P., Villaume, S., Rabenoelina, F., Schwarzenberg, A. & Nguema-Ona, E. et al. (2020) Bacillus subtilis and Pseudomonas fluorescens Trigger Common and Distinct Systemic Immune Responses in Arabidopsis thaliana Depending on the Pathogen Lifestyle. *Vaccines*, 8(3).

Nickstadt, A., Thomma, B.P.H.J., Feussner, I., Kangasjärvi, J., Zeier, J. & Loeffler, C. et al. (2004) The jasmonate-insensitive mutant jin1 shows increased resistance to biotrophic as well as necrotrophic pathogens. *Molecular Plant Pathology*, 5(5), 425–434.

Nie, P., Li, X., Wang, S., Guo, J., Zhao, H. & Niu, D. (2017) Induced Systemic Resistance against Botrytis cinerea by Bacillus cereus AR156 through a JA/ET- and NPR1-Dependent Signaling Pathway and Activates PAMP-Triggered Immunity in Arabidopsis. *Frontiers in Plant Science*, 8, 238.

Niu, D.-D., Liu, H.-X., Jiang, C.-H., Wang, Y.-P., Wang, Q.-Y. & Jin, H.-L. et al. (2011) The plant growth-promoting rhizobacterium Bacillus cereus AR156 induces systemic resistance in Arabidopsis thaliana by simultaneously activating salicylate- and jasmonate/ethylene-dependent signaling pathways. *Molecular Plant-Microbe Interactions: MPMI*, 24(5), 533–542.

Paauw, M., van Hulten, M., Chatterjee, S., Berg, J.A., Taks, N.W. & Giesbers, M. et al. (2023) Hydathode immunity protects the Arabidopsis leaf vasculature against colonization by bacterial pathogens. *Current Biology: CB*, 33(4), 697-710.e6.

Peterson, S.B., Dunn, A.K., Klimowicz, A.K. & Handelsman, J. (2006) Peptidoglycan from Bacillus cereus mediates commensalism with rhizosphere bacteria from the Cytophaga-Flavobacterium group. *Applied and Environmental Microbiology*, 72(8), 5421–5427.

Pfeilmeier, S., Petti, G.C., Bortfeld-Miller, M., Daniel, B., Field, C.M. & Sunagawa, S. et al. (2021) The plant NADPH oxidase RBOHD is required for microbiota homeostasis in leaves. *Nature Microbiology*, 6(7), 852–864.

Pfeilmeier, S., Werz, A., Ote, M., Bortfeld-Miller, M., Kirner, P. & Keppler, A. et al. (2024) Leaf microbiome dysbiosis triggered by T2SS-dependent enzyme secretion from opportunistic Xanthomonas pathogens. *Nature Microbiology*, 9(1), 136–149.

Pieterse, C.M., van Wees, S.C., van Pelt, J.A., Knoester, M., Laan, R. & Gerrits, H. et al. (1998) A novel signaling pathway controlling induced systemic resistance in Arabidopsis. *The Plant Cell*, 10(9), 1571–1580.

Pieterse, C.M.J., Berendsen, R.L., Jonge, R. de, Stringlis, I.A., van Dijken, A.J.H. & van Pelt, J.A. et al. (2021) Pseudomonas simiae WCS417: star track of a model beneficial rhizobacterium. *Plant and Soil*, 461(1–2), 245–263.

Pieterse, C.M.J., van Wees, S.C.M., Hoffland, E., van Pelt, J.A. & van Loon, L.C. (1996) Systemic Resistance in Arabidopsis Induced by Biocontrol Bacteria Is Independent of Salicylic Acid Accumulation and Pathogenesis-Related Gene Expression. *The Plant cell*, 8(8), 1225.

Pieterse, C.M.J., Zamioudis, C., Berendsen, R.L., Weller, D.M., van Wees, S.C.M. & Bakker, P.A.H.M. (2014) Induced systemic resistance by beneficial microbes. *Annual Review of Phytopathology*, 52, 347–375.

Pozo, M.J., van der Ent, S., van Loon, L.C. & Pieterse, C.M.J. (2008) Transcription factor MYC2 is involved in priming for enhanced defense during rhizobacteria-induced systemic resistance in Arabidopsis thaliana. *The New Phytologist*, 180(2), 511–523.

Rekhter, D., Lüdke, D., Ding, Y., Feussner, K., Zienkiewicz, K. & Lipka, V. et al. (2019) Isochorismate-derived biosynthesis of the plant stress hormone salicylic acid. *Science (New York, N.Y.)*, 365(6452), 498–502.

Riedlmeier, M., Ghirardo, A., Wenig, M., Knappe, C., Koch, K. & Georgii, E. et al. (2017) Monoterpenes Support Systemic Acquired Resistance within and between Plants. *The Plant Cell*, 29(6), 1440–1459.

Rudrappa, T., Czymmek, K.J., Paré, P.W. & Bais, H.P. (2008) Root-secreted malic acid recruits beneficial soil bacteria. *Plant Physiology*, 148(3), 1547–1556.

Sang, M.K. & Kim, K.D. (2012) The volatile-producing Flavobacterium johnsoniae strain GSE09 shows biocontrol activity against Phytophthora capsici in pepper. *Journal of Applied Microbiology*, 113(2), 383–398.

Schlaeppi, K. & Bulgarelli, D. (2015) The plant microbiome at work. *Molecular Plant-Microbe Interactions: MPMI*, 28(3), 212–217.

Schliep, K., Potts, A.J., Morrison, D.A. & Grimm, G.W. (2017) Intertwining phylogenetic trees and networks. *Methods in Ecology and Evolution*, 8(10), 1212–1220.

Shine, M.B., Gao, Q.-M., Chowda-Reddy, R.V., Singh, A.K., Kachroo, P. & Kachroo, A. (2019) Glycerol-3-phosphate mediates rhizobia-induced systemic signaling in soybean. *Nature Communications*, 10(1), 5303.

Simpson, E.H. (1949) Measurement of Diversity. *Nature*, 163(4148), 688.

Sohrabi, R., Paasch, B.C., Liber, J.A. & He, S.Y. (2023) Phyllosphere Microbiome. *Annual Review of Plant Biology*, 74, 539–568.

Soltani, A.-A., Khavazi, K., Asadi-Rahmani, H., Omidvari, M., Abaszadeh Dahaji, P. & Mirhoseyni, H. (2010) Plant Growth Promoting Characteristics in Some Flavobacterium spp. Isolated from Soils of Iran. *Journal of Agricultural Science*, 2(4).

Song, J.T., Lu, H., McDowell, J.M. & Greenberg, J.T. (2004) A key role for ALD1 in activation of local and systemic defenses in Arabidopsis. *The Plant Journal*, 40(2), 200–212.

Spellerberg, I.F. & Fedor, P.J. (2003) A tribute to Claude Shannon (1916–2001) and a plea for more rigorous use of species richness, species diversity and the 'Shannon–Wiener' Index. *Global Ecology and Biogeography*, 12(3), 177–179.

Spoel, S.H., Koornneef, A., Claessens, S.M.C., Korzelius, J.P., van Pelt, J.A. & Mueller, M.J. et al. (2003) NPR1 modulates cross-talk between salicylate- and jasmonate-dependent defense pathways through a novel function in the cytosol. *The Plant Cell*, 15(3), 760–770.

Stassen, M.J.J., Hsu, S.-H., Pieterse, C.M.J. & Stringlis, I.A. (2021) Coumarin Communication Along the Microbiome-Root-Shoot Axis. *Trends in Plant Science*, 26(2), 169–183.

Stringlis, I.A., Yu, K., Feussner, K., Jonge, R. de, van Bentum, S. & van Verk, M.C. et al. (2018) MYB72-dependent coumarin exudation shapes root microbiome assembly to promote plant health. *Proceedings of the National Academy of Sciences of the United States of America*, 115(22), E5213-E5222.

Teixeira, P.J.P., Colaianni, N.R., Fitzpatrick, C.R. & Dangl, J.L. (2019) Beyond pathogens: microbiota interactions with the plant immune system. *Current Opinion in Microbiology*, 49, 7–17.

Ton, J., van Pelt, J.A., van Loon, L.C. & Pieterse, C.M.J. (2002) Differential effectiveness of salicylate-dependent and jasmonate/ethylene-dependent induced resistance in Arabidopsis. *Molecular Plant-Microbe Interactions: MPMI*, 15(1), 27–34.

van de Mortel, J.E., de Vos, R.C.H., Dekkers, E., Pineda, A., Guillod, L. & Bouwmeester, K. et al. (2012) Metabolic and transcriptomic changes induced in Arabidopsis by the rhizobacterium Pseudomonas fluorescens SS101. *Plant Physiology*, 160(4), 2173–2188.

van Loon, L.C., Rep, M. & Pieterse, C.M.J. (2006) Significance of inducible defense-related proteins in infected plants. *Annual Review of Phytopathology*, 44, 135–162.

van Wees, S.C., Luijendijk, M., Smoorenburg, I., van Loon, L.C. & Pieterse, C.M. (1999) Rhizobacteria-mediated induced systemic resistance (ISR) in Arabidopsis is not associated with a direct effect on expression of known defense-related genes but stimulates the

expression of the jasmonate-inducible gene Atvsp upon challenge. *Plant Molecular Biology*, 41(4), 537–549.

Verhagen, B.W.M., Glazebrook, J., Zhu, T., Chang, H.-S., van Loon, L.C. & Pieterse, C.M.J. (2004) The transcriptome of rhizobacteria-induced systemic resistance in arabidopsis. *Molecular Plant-Microbe Interactions: MPMI*, 17(8), 895–908.

Vlot, A.C., Sales, J.H., Lenk, M., Bauer, K., Brambilla, A. & Sommer, A. et al. (2021) Systemic propagation of immunity in plants. *The New Phytologist*, 229(3), 1234–1250.

Vogel, C., Bodenhausen, N., Gruissem, W. & Vorholt, J.A. (2016) The Arabidopsis leaf transcriptome reveals distinct but also overlapping responses to colonization by phyllosphere commensals and pathogen infection with impact on plant health. *The New Phytologist*, 212(1), 192–207.

Vogel, C.M., Potthoff, D.B., Schäfer, M., Barandun, N. & Vorholt, J.A. (2021) Protective role of the Arabidopsis leaf microbiota against a bacterial pathogen. *Nature Microbiology*, 6(12), 1537–1548.

Wang, C., El-Shetehy, M., Shine, M.B., Yu, K., Navarre, D. & Wendehenne, D. et al. (2014) Free radicals mediate systemic acquired resistance. *Cell Reports*, 7(2), 348–355.

Wang, C., Liu, R., Lim, G.-H., Lorenzo, L. de, Yu, K. & Zhang, K. et al. (2018) Pipecolic acid confers systemic immunity by regulating free radicals. *Science Advances*, 4(5), eaar4509.

Wang, W., Withers, J., Li, H., Zwack, P.J., Rusnac, D.-V. & Shi, H. et al. (2020) Structural basis of salicylic acid perception by Arabidopsis NPR proteins. *Nature*, 586(7828), 311–316.

Wenig, M., Ghirardo, A., Sales, J.H., Pabst, E.S., Breitenbach, H.H. & Antritter, F. et al. (2019) Systemic acquired resistance networks amplify airborne defense cues. *Nature Communications*, 10(1), 3813.

Wilcoxon, F. (1945) Individual Comparisons by Ranking Methods. *Biometrics Bulletin*, 1(6), 80.

Wildermuth, M.C., Dewdney, J., Wu, G. & Ausubel, F.M. (2001) Isochorismate synthase is required to synthesize salicylic acid for plant defence. *Nature*, 414(6863), 562–565.

Wu, L., Huang, Z., Li, X., Ma, L., Gu, Q. & Wu, H. et al. (2018) Stomatal Closure and SA-, JA/ET-Signaling Pathways Are Essential for Bacillus amyloliquefaciens FZB42 to Restrict Leaf Disease Caused by Phytophthora nicotianae in Nicotiana benthamiana. *Frontiers in Microbiology*, 9, 847.

Yildiz, I., Gross, M., Moser, D., Petzsch, P., Köhrer, K. & Zeier, J. (2023) N-hydroxypipecolic acid induces systemic acquired resistance and transcriptional reprogramming via TGA transcription factors. *Plant, Cell & Environment*, 46(6), 1900–1920.

Yildiz, I., Mantz, M., Hartmann, M., Zeier, T., Kessel, J. & Thurow, C. et al. (2021) The mobile SAR signal N-hydroxypipecolic acid induces NPR1-dependent transcriptional reprogramming and immune priming. *Plant Physiology*, 186(3), 1679–1705.

Yilmaz, P., Parfrey, L.W., Yarza, P., Gerken, J., Pruesse, E. & Quast, C. et al. (2014) The SILVA and "All-species Living Tree Project (LTP)" taxonomic frameworks. *Nucleic Acids Research*, 42(Database issue), D643-8.

Yu, K., Soares, J.M., Mandal, M.K., Wang, C., Chanda, B. & Gifford, A.N. et al. (2013) A feedback regulatory loop between G3P and lipid transfer proteins DIR1 and AZI1 mediates azelaic-acid-induced systemic immunity. *Cell Reports*, 3(4), 1266–1278.

Zavaliev, R. & Dong, X. (2024) NPR1, a key immune regulator for plant survival under biotic and abiotic stresses. *Molecular Cell*, 84(1), 131–141.

Zavaliev, R., Mohan, R., Chen, T. & Dong, X. (2020) Formation of NPR1 Condensates Promotes Cell Survival during the Plant Immune Response. *Cell*, 182(5), 1093-1108.e18.

Zeier, J. (2021) Metabolic regulation of systemic acquired resistance. *Current Opinion in Plant Biology*, 62, 102050.

Zhu, L., Huang, J., Lu, X. & Zhou, C. (2022) Development of plant systemic resistance by beneficial rhizobacteria: Recognition, initiation, elicitation and regulation. *Frontiers in Plant Science*, 13, 952397.

SUPPORTING INFORMATION

Additional supporting information can be found online in the Supporting Information section at the end of this article.

How to cite this article: Sommer, A., Wenig, M., Knappe, C., Kublik, S., Foesel, B.U., Schloter, M. et al. (2024) A salicylic acid-associated plant-microbe interaction attracts beneficial *Flavobacterium* sp. to the *Arabidopsis thaliana* phyllosphere. *Physiologia Plantarum*, 176(4), e14483. Available from: https://doi.org/10.1111/ppl.14483